Examining Solution and Solid State Composition for the Solution Mediated Polymorphic Transformation of Carbamazepine and Piracetam

Marcus A. O'Mahony, Anthony Maher ǂ , Denise M. Croker ǂ, Åke C. Rasmuson ǂ, Benjamin K. Hodnett .*

* ǂ Solid State Pharmaceutical Cluster, Materials and Surface Science Institute, Department of Chemical and Environmental Sciences, University of Limerick, Limerick, Ireland.

*corresponding author email: marcus.omahony@ul.ie

*Tel.: +353 61 234160

ABSTRACT

Solution mediated polymorphic transformations (SMPT) of the pharmaceutical compounds carbamazepine and piracetam have been investigated. Seeded transformation experiments were performed, and the solution concentration was monitored by *in situ* infra-red spectroscopy using a calibration free method. Solid samples were also taken over time, and the percentage of metastable and stable polymorphic phases were determined using off line quantitative powder X-ray diffraction analysis. Solution and solid state data were compared for each compound. In the case of carbamazepine, the SMPT from FI to FIII was identified as being controlled by the growth of the stable FIII polymorph. For piracetam, the SMPT was also identified as being controlled by growth of the stable polymorph, but

with a more considerable induction time for nucleation of the stable phase. This paper demonstrates how the rate determining steps of the SMPT can be identified if both solution and solid phase data are recorded. The results are compared with other studies reported in the literature and rationalized into four principal scenarios.

INTRODUCTION

Crystallization is regularly used for the isolation of a desired chemical product from solution. The isolated crystalline product can often form more than one crystal structure, despite identical chemical compositions. This is known as polymorphism. Different polymorphs have different arrangements of their molecules within their crystal structure giving rise to differences in free energy. These differences in free energy relates directly to the observed differences in physical properties for each polymorph, e.g. solubility, dissolution rates, melting points, densities, particle habits [1] Thus, isolation of the desired polymorphic form is of utmost importance for chemical product manufacture and performance. Where a metastable polymorph has crystalized first and continues to interact with a bulk solvent phase, the potential can exist for a transformation to the more stable polymorph to occur by a process of dissolution and crystallization. This is known as a solution mediated polymorphic transformation (SMPT) and can be used to isolate the most stable polymorphic form [2, 3]. In the context of selecting the desired polymorph, understanding and monitoring these transformations is of immediate importance to the chemical industry and in particular to pharmaceutical manufacture.

With the advent of Process Analytical Technology in situ monitoring of solution mediated polymorphic transformations is now possible [4, 5]. Attenuated Total Reflectance Fourier Transform Infra-Red spectroscopy (ATR-FTIR) has been adapted to accommodate *in situ* monitoring of solution concentrations during crystallizations [6]. The extent of supersaturation in the solution, during a crystallization experiment, can be monitored by relating solute peak height or area from ATR-FTIR to solution concentration. Partial least squares models [7] are typical but more recently, a calibration free

method [8] has been successfully implemented. The work undertaken here uses a calibration free method to monitor *in situ* solution concentration/supersaturation over time.

Monitoring solution concentration/supersaturation over time for SMPTs enables evaluation of the kinetics of the transformation under the theoretical framework originally developed in the landmark paper by Cardew and Davey [9]. By observation of the de-supersaturation profile over time it is possible to establish whether the transformation is controlled by the dissolution of the metastable form or growth of the stable form. This has been demonstrated numerous times for polymorphs and hydrates [10-12]. It is worth noting that this framework does not account for the nucleation of the stable phase during solution mediated transformations. To date, there is some data in the literature for SMPT where the solution concentration/supersaturation data is presented in conjunction with polymorph composition data. In a study by Kelly and Rodriguez-Hornedo, solution and solid state data were presented for the SMPT of FII to FIII carbamazepine [13]. The dissolution of the metastable FII or growth of the stable FIII could be identified as the controlling step in the transformation, depending on the solvent used in crystallization experiments. In seeded SMPT experiments performed by Scholl et al. the transformation from the α to the β form of L-glutamic acid was monitored using in situ solution and solid state analysis techniques. The results showed that the transformation to the β polymorph was controlled by the growth of the β polymorph during the transformation [4]. A most recent study by Thirunahari et al. monitored a seeded SMPT experiment using *in situ* ATR-FTIR and Raman spectroscopy to monitor the solution and solid states, respectively [14]. It was found that for the transformation from the metastable form I^L to the stable form II polymorph of tolbutamide a considerably long induction time preceded the transformation. Following this induction time the SMPT was controlled by the dissolution of the metastable polymorph. The authors concluded that the nucleation of the stable polymorph was the controlling step in the transformation.

Carbamazepine (benzo[b][1]benzazepine-11-carboxamide) is a pharmaceutical compound known to have five polymorphic forms (FI, FII, FIII, FIV and FV), a dihydrate form and a range of solvates and co-crystals [15]. FII has recently been found to be a channel solvate [16, 17] FIV [18] and FV [19] are formed via templated growth from a polymeric substrate and single crystal of dihydrocarbamazepine, respectively. FIII, the P-monoclinic form, is the most thermodynamically stable form of carbamazepine at room temperature. FI, the triclinic form, is enantiotropically related to FIII with a transition temperature of 78 °C [20]. Below this temperature FIII is stable and above 78 °C FI is stable. FI is typically formed at temperatures above 130 °C via a solid-gas-solid conversion [21]. In this study, the solution mediated polymorphic transformation of FI to FIII carbamazepine (CBZ) was examined in methanol at 10 °C.

Piracetam (2 – oxo – 1 – pyrrolidine acetamide) is another polymorphic pharmaceutical compound with five reported polymorphs. Two of these polymorphs (FIV and FV) are only obtained at pressures greater than 0.5 GPa [22]. FI, FII and FIII Piracetam (PCM) have been identified and structurally characterized under ambient pressures [23]. FI is formed by heating FII or FIII to 127 °C and then quench cooling to room temperature. FI is highly unstable as it readily transforms to FII within a few hours under ambient conditions. FII is metastable, and FIII is the stable polymorph, as determined by melting points. Kuhnert-Brandstatter et al. claim that FII and FIII also have an enantiotropic relationship with a transition temperature above 75 °C [24], but no experimental evidence exists to verify this claim. The solubility of FIII has been determined by Maher et al. [25]. Cooling crystallizations have shown the selection of FII or FIII PCM based on the solvent used [26]. In other studies using in situ energy dispersive X-ray diffraction, all three polymorphs were identified during cooling crystallizations with multiple solvents. FI formed initially but had a short lifetime and transformed to FII and/or FIII with continued cooling [27]. The FI polymorph of PCM was not seen for the transformation experiments performed here. In this study, the solution mediated polymorphic transformation of FII to FIII PCM was monitored in ethanol at 50 °C.

EXPERIMENTAL SECTION

Preparation of Polymorphs

Pharmaceutical grade carbamazepine was obtained from POLPHARMA S.A. (Starogard Gdański, Poland) and stored over silica gel (0% humidity) between 2-8 °C. Piracetam was supplied by AXO Industry Ltd. and complies with European Pharmacopoeia standards (CAS number: 7491-74-9). ACS reagent grade methanol and ethanol were used having a purity of ≥99.8 % and 99.9 %, respectively.

The FIII polymorph of CBZ was prepared by crystallization from ethanol. Using the Mettler-Toledo LabMaxTM automatic lab reactor, 36.9 g of pharmaceutical grade CBZ was dissolved in 393 g of ethanol at 78 °C and held for 1 hr under reflux. The solution was cooled at 1 °C / min to 20 °C and aged for 15 hrs. Further cooling was then applied at 1 °C / min to 10 °C and the solution was aged for 8 hrs. The solids were harvested using vacuum filtration and dried at 25 °C under vacuum for approximately 40 mins, using a vacuum oven. Later, these solids were suspended in excess in ethanol under vigorous magnetic stirring to reduce the particle size. This was necessary to reduce the effects of preferred orientation for FIII CBZ in powder X-ray diffraction (PXRD) analysis.

To prepare the FI CBZ polymorph, 3 g of pharmaceutical grade CBZ powder was placed on a large clock glass. This was then placed on aluminium foil and covered by a large glass cover. Aluminium foil was also placed on top of the cover before heating the CBZ powder in the oven at 145°C for 2.5 hrs under vacuum. Thereafter, the pressure was adjusted to ambient and the powder was held in the oven for 15-20 mins. The powder was allowed to cool slowly to 100°C before removing from the oven and placing in a dessicator for cooling to room temperature.

The FIII polymorph of PCM was produced from a cooling crystallization in methanol; 336 g of the commercial product was dissolved over 2 hrs. in 700 g of methanol at 60 °C in a Mettler-Toledo LabMaxTM. The solution was cooled at 0.1 °C / min to 20 °C, agitated for 4 h, and cooled further at 0.1

°C / min to 5 °C and agitated for a further 10 h. The solids were isolated using vacuum filtration, washed once with a small amount of propanol, and held at 55 °C overnight to dry.

The FII polymorph of PCM was produced by heating the prepared FIII. 10 g of FIII was ground to a fine powder and placed in an oven at 140 °C for 3 days, with occasional mixing. The powder was removed from the oven and allowed to cool to room temperature.

The polymorphic form of each pharmaceutical compound was confirmed using PXRD (Panalytical X'Pert MPD PRO). Their respective polymorphic purity was confirmed by comparison to the theoretical PXRD pattern generated from the crystallographic information file for each structure (CCDC reference codes: FI CBZ-CBMZPN11, FIII CBZ-CBMZPN10, FII PCM-BISMEV, FIII PCM-BISMEV01). The individual polymorphs were imaged using a Joel CarryScope JCM-5700 scanning electron microscope (SEM).

Quantification of Polymorphic Mixtures

Individual calibration standards containing varying amounts of FI and FIII CBZ, and FII and FIII PCM, were weighed out to a total mass of 0.2 g. The respective standards were mixed by grinding gently in an agate motor and pestle for ~1min. The calibration standards were then placed on a zero background disk and scanned from 3-33 °2θ for CBZ polymorphs and 8-35 °2θ for PCM polymorphs with wavelength 1.541Å (40kV, 35mA). The diffracting radiation was collected using an X'celerator detector. The samples were also rotated during data collection to reduce the effects of preferred orientation. Analysis of the PXRD scan data was completed using X'Pert HighScore Plus software. Solid samples collected during transformation experiments were also analysed in this way.

The integrated peak areas of stable FIII CBZ peaks at 15.1 and 15.4 °2θ and metastable FI CBZ peaks between 3-10 °2θ were used to calculate the relative amounts of each polymorph in a mixture of the two forms. The same method was used to calculate the relative amounts of metastable FII and stable FIII PCM using the peaks at 17.5 and 26 °2θ, respectively. In each case, calculation of % peak area of the

stable polymorph was achieved by dividing the peak area of the stable polymorph by the sum of the peak area of the metastable and stable polymorphs and expressing it as a percentage [28]. The % peak area of the metastable polymorph was then the remaining percentage in the mixture. Correlation curves were constructed from the % peak area of the stable polymorph measured by PXRD and the % w/w polymorph in the mixture.

CBZ and Methanol: Solution Concentration Monitoring

The solution concentration behaviour of CBZ in methanol was monitored qualitatively over time during the transformation with *in situ* ATR-FTIR (ReactIR iC10 with DiComp probe with silver halide fibre) using a calibration free method [8]. The intensity of the Infra-red absorption of the C=O stretch of CBZ in solution, represented by peak height or peak area, is proportional to its concentration [29]. This was used to monitor the concentration in solution during the transformation. In practice the ratio of the CBZ carbonyl absorbance at 1680cm^{-1} to the at methanol peak at 1120cm^{-1} (overtone band) was used as the signal to noise ratio for the CBZ carbonyl absorbance in methanol was quite weak. An ATR-FTIR measurement was taken every 30 s in the range from 650cm^{-1} to 1800cm^{-1} using iCIR software. A 100 mL jacketed glass vessel with magnetic stirring was used in conjunction with a Lauda E305 recirculator and E300 controller to ensure a constant temperature during the experiments. Methanol was pre-saturated with 4.95 g CBZ in 100 mL such that the solvent was almost saturated with respect to stable FIII CBZ polymorph at 10 °C. The solution was heated to 20 °C for 1hr, to ensure all the solid phase had dissolved, and then cooled to 10 °C and held for 30mins prior to the addition of 2.70 g FI CBZ solids.

Once the FI solids had been added and where the solution reached its plateau concentration, measured by ATR-FTIR during the transformation, a solution sample was taken to gravimetrically determine the solubility of FI CBZ in methanol at 10°C. At this point, FTIR data collection was paused and the stirring was switched off to allow the suspended solid to settle. A solution sample was carefully filtered into a pre-weighed vial and then weighed to determine the solution mass. After drying, the remaining solute

was weighed and the concentration was expressed as g solute / g solvent. FIII CBZ solubility was determined in a similar manner.

PCM and Ethanol: Solution Concentration Monitoring

The solution concentration behaviour of PCM in ethanol was monitored over time during the transformation using the same ATR-FTIR measurements described above. Monitoring only the peak area absorbance at 1680cm^{-1} (C=O stretch) was necessary as the carbonyl absorbance for PCM in ethanol was quite strong. A 250 mL jacketed vessel with overhead stirring was used with the same recirculator and controller as described above. Ethanol was pre-saturated with 16.23 g PCM in 165mL such that the solvent was saturated with respect to the stable FIII PCM polymorph at 50 °C. The solution was preheated to 60 °C for 30mins and then cooled to the experimental temperature of 50 °C and held for another 30mins prior to the addition of 3.28 g of FII solids.

FII PCM solubility was determined separately by slurrying FII PCM in excess in contact with ethanol. Over time, the solid phase was monitored by PXRD. At the point where FIII PCM solid had just appeared in the solid phase a solution sample was taken to gravimetrically determine the solution concentration (as above). This was taken as the solubility of FII PCM. FIII PCM solubility has been determined elsewhere [25].

Solid Phase monitoring

In both experiments, the solid phase was also monitored during the transformation by filtering some of the excess solid, at selected times, through a 0.22μm membrane using an Hirsch funnel under vacuum. It was assumed that this did not affect the concentration profile during the experiment as the sample taken was quite small (50-100 mg) and the reactor contents were well mixed. The dry solid was kept in a dessicator and later analysed by PXRD to determine the polymorphic composition during the solution mediated transformation.

The polymorphic forms of CBZ - FI and FIII, and PCM - FII and FIII were identified by PXRD, as shown in Figure 1 and 2, respectively. Both polymorphic forms agree well with the theoretical patterns and with those reported in the literature [24, 30]. The habit of each polymorph is also illustrated by the SEM images seen in Figure 3.

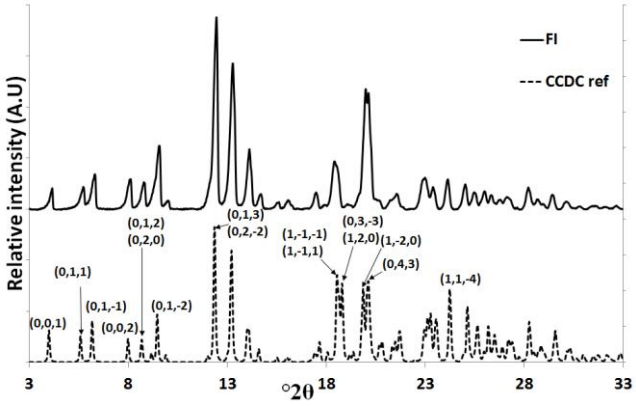

(a)

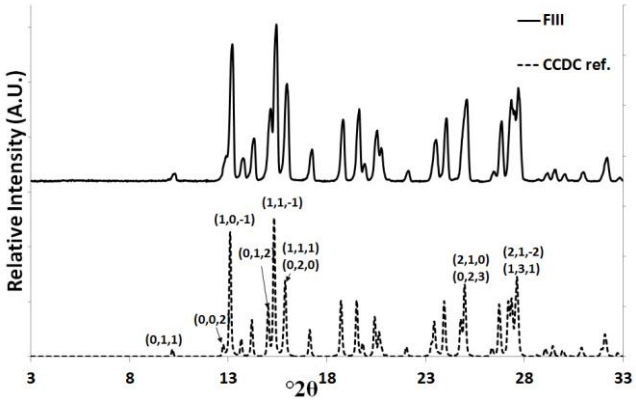

(b)

Figure 1. (a) FI CBZ PXRD pattern compared to the theoretical PXRD pattern of FI CBZ with peaks indexed. (b) FIII CBZ PXRD pattern compared to the theoretical PXRD pattern of FIII CBZ with peaks indexed.

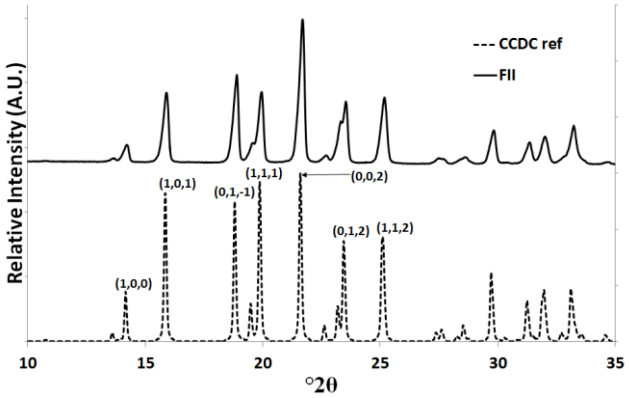

(a)

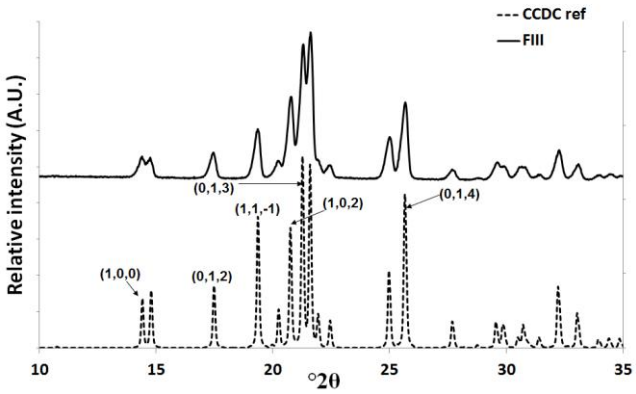

(b)

Figure 2. (a) FII PCM PXRD pattern compared to the theoretical PXRD pattern of FII PCM with peaks indexed. (b) FIII PCM PXRD pattern compared to the theoretical PXRD pattern of FIII PCM with peaks indexed.

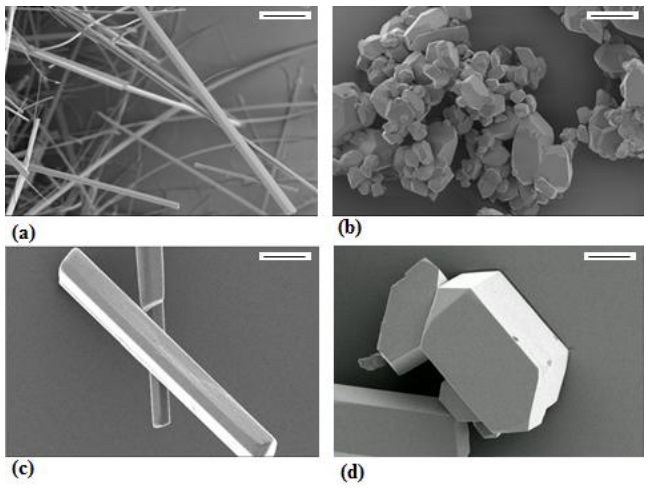

Figure 3. SEM images for each polymorphic form of CBZ and PCM. (a) highly acicular FI CBZ, (b) granular FIII CBZ, (c) rod like FII PCM and (d) prismatic FIII PCM. Inset: scale bar 50µm.

The correlation curves for the calculated % peak area of polymorph versus actual % w / w polymorph of FIII CBZ and FIII PCM are shown in Figures 4 and 5, respectively. Both correlation curves show an R^2 value close to 1 illustrating a good fit between calculated amounts and actual amounts present in % w /w. Scatter in the data results in an offset in % w/w from 100% and 0% area for each of the calibration curves. This offset relates to the specification of the baseline in the peak area determination (automatically determined by the HighScore software program). Subsequent solid samples measured during the SMPT experiments are normalized to show 0% and 100% of the stable polymorph when these % areas are calculated.

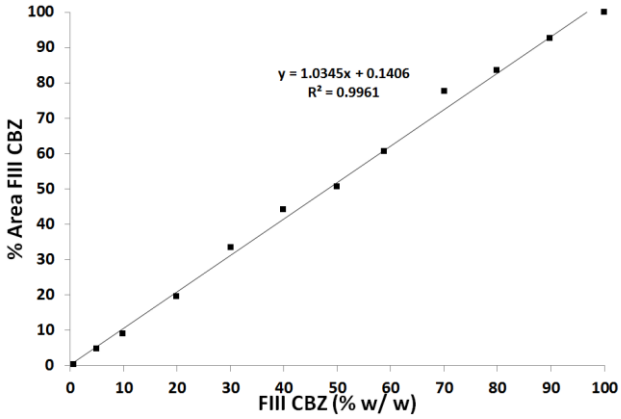

Figure 4. Correlation curve illustrating the relationship between the mass of FIII CBZ polymorph and the calculated % area of FIII CBZ polymorph in a mixture of FI and FIII CBZ polymorphs, as measured by PXRD.

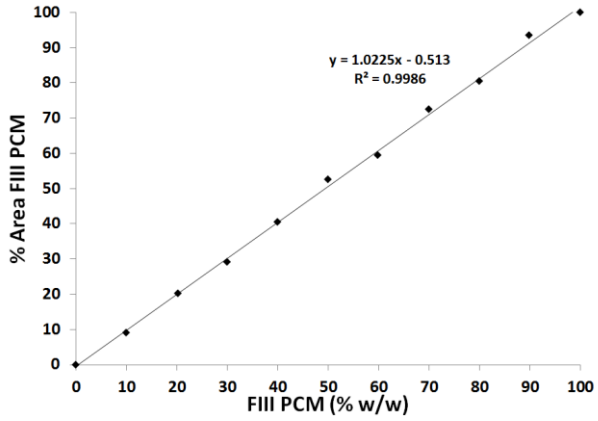

Figure 5. Correlation curve illustrating the relationship between the mass of FIII PCM polymorph and the calculated % area of FIII PCM polymorph in a mixture of FII and FIII PCM polymorphs, as measured by PXRD.

The solubility of the stable and metastable solid forms of both CBZ and PCM is presented in Table 1. The most stable polymorph will have the lowest solubility and this is seen for both systems. The data illustrate that there is a small but significant difference in solubility between the polymorphs.

Table 1. Polymorph Solubility data with standard deviations (n=3) for polymorphs of carbamazepine and piracetam at 10 °C and 50 °C, respectively.

	Carbamazepine at 10 °C (g_{CBZ} / $g_{methanol}$)		**Piracetam at 50 °C (g_{PCM} / $g_{ethanol}$)**		**Solubility Ratio**
Solvent	FI	FIII	FII	FIII	
Ethanol			0.1281 (±0.0001)	0.1248 (±0.0001)	1.03
Methanol	0.0874 (±0.0001)	0.0630 (±0.0001)			1.39

The metastable polymorphs of both CBZ and PCM are quite stable in the solid state and do not undergo structural changes in the absence of solvent. Both FI CBZ and FII PCM have been stored as dry solids in excess of one year without transformation. Suspension of the metastable FI polymorph of CBZ in methanol at 10 °C resulted in transformation to the stable FIII polymorph of CBZ. Similarly, suspension of metastable FII polymorph of PCM in ethanol at 50 °C resulted in transformation to the stable FIII polymorph of PCM. In Figure 6 and 7 solid state compositions and the solution concentrations for the SMPT for CBZ FI to FIII and PCM FII to FIII are presented. The *in situ* ATR-FTIR peak area absorbance is directly proportional to solution concentration and this is plotted in each figure. Solid samples were also taken at different time points during each SMPT and the % of each polymorph in the solid phase was determined.

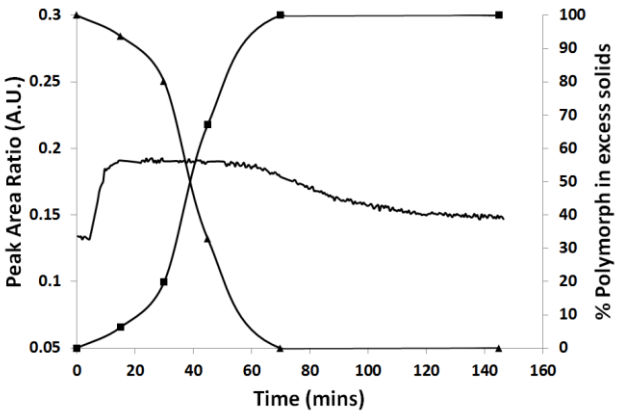

Figure 6. Solution mediated polymorphic transformation of FI to FIII CBZ in methanol at 10 °C. The solution concentration profile, as measured by *in situ* ATR-FTIR, and polymorphic composition as measured by PXRD, are indicated. ■ % FIII CBZ polymorph, ▲ % FI CBZ polymorph. In the case of the polymorphic composition data the lines are added as guide for the eye.

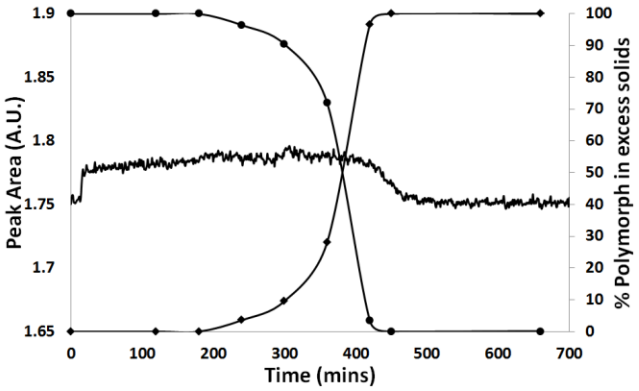

Figure 7. Solution mediated polymorphic transformation of FII to FIII PCM in ethanol at 50 °C. The solution concentration profile, as measured by *in situ* ATR-FTIR, and polymorphic composition, as measured by PXRD, are indicated. ♦ % FIII PCM polymorph, ● % FII PCM polymorph. In the case of the polymorphic composition data the lines are added as guide for the eye.

In both SMPTs, addition of the metastable solid polymorph to each solution resulted in a step increase in solution concentration. This indicated the fast dissolution of the metastable polymorph which resulted in the solution becoming saturated with respect to the metastable polymorph and supersaturated with respect to the stable polymorph. Over time, nucleation and then growth of the stable polymorph occurred at the expense of the dissolving metastable polymorph. Where the total rate of growth is compensated for by the much faster total rate of dissolution, a plateau in solution concentration/supersaturation is achieved and this has been previously identified by Cardew and Davey [9]. The evidence of a plateau region in both of the SMPT experiments presented here showed that the transformations were controlled by growth of the stable polymorph. Once all of the metastable polymorph had dissolved, the stable polymorph continued to grow until it was in equilibrium with the solution.

In Figure 6, the polymorphic transformation of FI to FIII CBZ in methanol at 10 °C is shown. Monitoring the polymorphic composition shows that the transformation has established itself after 15mins with some stable FIII CBZ detectable by PXRD. The solid phase completely transformed to the stable FIII CBZ polymorph after 70mins. The solution concentration did not reach equilibrium with FIII CBZ until 120mins.

Figure 7 shows the polymorphic transformation of FII to FIII PCM in ethanol at 50°C. The transformation was much slower than that observed for CBZ polymorphs, despite the higher temperature of the experiment. The transformation to the stable FIII PCM polymorph only appears to have initiated after 180mins (as detected by PXRD). The solid phase had completely transformed to the stable FIII PCM polymorph after 450mins and the solution did not reach equilibrium with the FIII PCM polymorph until 500mins. It should be noted that the solubility difference between the polymorphs of PCM is quite smaller than that of CBZ. As a result much smaller differences are observed with ATR-FTIR in the solution concentration making the data appear rougher. Periodic addition of liquid nitrogen to the ATR-FTIR instrument over longer periods of time is required to keep it cool. The appearance of a slight upward drift in plateau region of the data can be explained due to the long transformation time and the slight heating of the instrument over time.

For the SMPT of PCM and CBZ polymorphs, it is important to note that the solution concentration remains at the solubility of the metastable polymorph for quite some time after the stable polymorph has nucleated and grown. Decay in solution concentration only occurs when essentially all of the metastable polymorph has dissolved.

DISCUSSION

A solution mediated transformation proceeds via three identifiable processes: nucleation of the stable phase, growth of the stable phase and dissolution of the metastable phase. These processes are at play to produce the rate at which a transformation proceeds. The solution concentration profiles for this work show a plateau region for the solution concentration over time. For the SMPT of CBZ, solid state data showed that the stable FIII polymorph nucleated and grew readily in the solution during the plateau region where the solution was supersaturated with respect to FIII CBZ. However, for the SMPT of PCM there was a considerable lag time of approx. 180mins prior to the nucleation and growth of FIII PCM in the plateau region. This lag or induction time, detected by PXRD, is often assumed to be inversely proportional to the nucleation rate [31]. This shows that nucleation appears to play a significant role in determining the transformation time for FII to FIII PCM. For the case of the SMPT of FI to FIII CBZ, nucleation appears to take place very early during the process, and a lag time cannot be established.

The induction time (nucleation) of the stable polymorph was also a considerable factor in determining the transformation time for a recently published experiment involving the SMPT of tolbutamide form I^L to form II [14]. This transformation experiment was performed by saturating an ethanol/water solution with enough tolbutamide so it was saturated with respect to the metastable form I^L. Then seeds of form I^L were suspended in contact with this saturated solution and the SMPT was monitored over time. One of the interesting features of this transformation is that during the plateau region in the solution concentration profile no nucleation and growth of the stable form II polymorph could be detected. Once the form II polymorph nucleated the solution concentration dropped rapidly as the stable form II polymorph grew. This demonstrated that the total rate of growth was much faster than the total rate dissolution and that once nucleation occurred, the transformation to the stable phase was only controlled by dissolution of the metastable polymorph. The plateau in solution concentration resulted due to the induction time required to nucleate the stable form II polymorph and not because dissolution was

comparatively more rapid than growth [9]. A very similar SMPT experiment was performed in the case of L-glutamic acid [4] where seeds of the metastable α form were added to a solution that was saturated with respect to the metastable α form. Interestingly, in contrast to the case of tolbutamide, during the plateau region of the solution concentration profile the stable β polymorph was seen to nucleate and grow immediately without any measurable induction time for nucleation (similar to the case of the CBZ FI to FIII SMPT presented above).

Combining these experimental data already present in the literature with those of this work, it is clear that four principal scenarios appear possible for solution mediated polymorphic transformations. In the schematic diagrams below these scenarios are sketched with the solution and solid state data considered in combination.

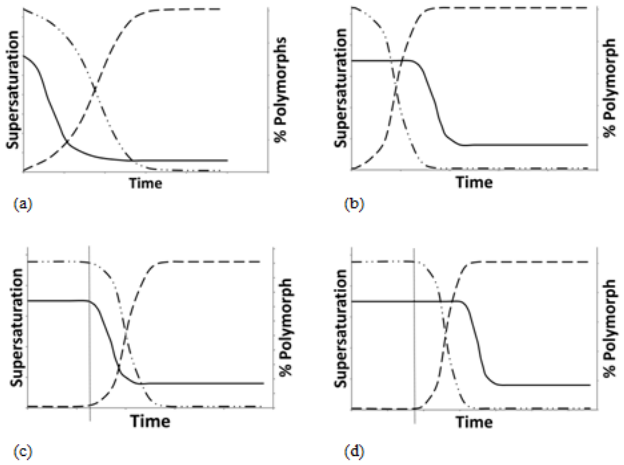

Figure 8. Representations of possible scenarios for solution mediated polymorphic transformations given solution concentration/supersaturation profiles and solid state compositions. − solution/supersaturation profile, - - - stable phase composition and −•• metastable phase composition. Vertical line indicates limit of the induction time for nucleation of the stable phase.

In (a) and (b) of Figure 8, the theoretical basis for the observed solution concentration/supersaturation profiles and solid state data has been established [9]. In both scenarios there is a very short induction time

before the stable solid phase (e.g. polymorph, hydrate, etc.) appears, i.e. the nucleation of the stable phase is quite rapid. In scenario (a) the solution concentration drops immediately after any appreciable amount of the stable phase has been produced. This signifies that the consumption of supersaturation by growth [g/L.s] is fast compared to the overall rate of dissolution [g/L.s] of the metastable solid phase. This is denoted as a "dissolution controlled polymorphic transformation". From a simple mechanistic point of view, the overall rates of dissolution and growth [g/L.s] are governed by the driving force, the total solid-liquid interfacial surface area, and the mass transfer/surface integration rate constant. The intrinsic rate of dissolution [g/m^2.L.s] is normally assumed to be higher than the corresponding intrinsic rate of growth [g/m^2.L.s] since the latter often involves a surface integration resistance in addition to the boundary layer transport resistance. If we rule out major differences in the rate constants case (a) is then expected to primarily illustrate the situation when the interfacial solid-liquid surface area of the metastable form is much smaller over most of the transformation time than that of the stable form. For example, this can occur if the metastable form is composed of a relatively small number of large crystals and the nucleation results in a significant number of crystals (nuclei) of the stable form.

In scenario (b), the solution concentration stays at the solubility of the metastable form for quite some time so that a plateau is established, and moreover, the plateau extends until almost no metastable solid form remains in the suspension. In this scenario the rate of consumption of supersaturation [g/L.s] by crystal growth of the stable form, over most of the transformation, is clearly lower than the overall rate of dissolution [g/L.s] of the metastable form. This case is denoted as "growth controlled polymorphic transformation". We would expect that this situation is more common than scenario (a), since the intrinsic rate of growth is expected to be lower than the intrinsic rate of dissolution. Otherwise, the same considerations over the influence of the solid-liquid interfacial surface areas apply for this case. It should be clearly recognised that the initial total surface area of the metastable form can be well controlled in the experiment, while the total surface area of the stable form is entirely governed by the number of crystals that are nucleated of that form, and with the present state of knowledge we have very little control over this.

Insofar as the solid state data is in line with the diagrams in Figure 8 (a) and (b), the solution/supersaturation profiles reflect a situation where the solution mediated transformation process is controlled by the dissolution of the metastable phase or by the growth of the stable phase, respectively. Experimental evidence for this behaviour is seen in the literature [4, 9, 13, 32]. On this basis, the SMPT for FI to FIII CBZ in this work is controlled by growth of the stable FIII polymorph – scenario (b).

Scenario (c) of Figure 8 is similar to scenario (a) in that the solution concentration drops quite rapidly as soon as the stable phase starts to form. From that point of view it would be classified as a dissolution controlled process. However, the difference to scenario (a) is that the nucleation of the stable form exhibits an induction time which leads to the solution concentration being maintained at the solubility of the metastable form for quite some time, allowing a plateau region to be created. The difference to scenario (b), however, is that in scenario (c) very little is actually happening during most of that plateau region, since there is of course no transformation occurring until the stable phase has nucleated. Once it has nucleated, the rate of transformation is essentially limited by the rate of dissolution, for the same reasons as discussed for scenario (a). We would like to classify this case as a "nucleation-dissolution controlled polymorphic transformation", and the characteristic features are a plateau region in the solution concentration as well as an unchanging single solid phase, and the fact that the solution concentration starts to decay only as the transformation is initially detected in the solid phase data. Of course in the absence of solid phase information, it would not be possible to distinguish scenario (c) from scenario (b). As has been seen in the case of tolbutamide [14], this scenario (c) is possible where the induction time for nucleation of the stable phase is responsible for the plateau region in the SMPT profile. Thereafter, the SMPT is controlled by dissolution of the metastable phase.

The final case is illustrated by Figure 8(d), which resembles scenario (c) in that there is a plateau region in the solution concentration as well as an unchanging single solid phase. Similar to scenario (c), there is an induction time prior to any of the stable form being detected. However, different to scenario (c) is that in scenario (d) the solution concentration does not start to decay until most of the metastable

form has transformed to the stable form. Accordingly, the overall growth rate is clearly slower than the overall dissolution rate, for the same reasons as was discussed for case (b). We would like to name scenario (d) as a "nucleation-growth controlled polymorphic transformation" This scenario is been exemplified in SMPT experiments involving the compounds taltireline [33], glycine [34] and for the SMPT of FII to FIII Piracetam presented here.

It is worth considering that the four principal scenarios described in Figure 8 could also be determined on the basis of nucleation behavior alone. On the assumption that the intrinsic rate of dissolution is greater than the intrinsic rate of growth (established previously in the text) the resultant scenario for SMPT should depend only on the nucleation behaviour. That is, when nucleation of the stable phase occurs and whether or not the nucleation of the stable phase results in a relatively large or small number of nuclei. The former has the effect as to whether or not an induction time will be detected whereas the latter will be a key determinant in the interfacial solid-liquid surface area of the stable phase available for growth. The four scenarios can be rationalised in terms of combinations of this nucleation behaviour. If the nucleation occurs quickly, without the detectable presence of an induction time, with a prolific number of nuclei being present the interfacial solid-liquid surface area of the stable form is much higher than that of the metastable form over most of the transformation time. As a result, total growth rate of the stable phase will be ample so as to make the dissolution of the metastable phase the controlling step and this will result in scenario (a). If nucleation occurs quickly but the number of nuclei present is scarce the interfacial solid-liquid surface area of the stable phase is reduced and thus the total growth rate of the stable phase will also be reduced. This will result in the growth of the stable phase being the controlling step in the transformation. This is identified by scenario (b). In the case where nucleation does not occur quickly and there is a detectable induction time, the scenario that will result is again dependent on whether the number of nuclei that are present are in abundance or scarce. Scenario (c) and (d) have induction times for the appearance of the stable phase and thereafter are the same as that of scenarios (a) and (b), respectively. Allowing for the possibility of a detectable induction time, the boundaries between

the different scenarios will depend on the growth rate of the stable phase which is directly influenced by the number of crystals of the stable phase that nucleate.

Experimental evidence for the scenarios described in Figure 8 is presented in Table 2 in more detail. For each of the SMPT experiments listed, both solution and solid state data are presented. Accordingly, the classification for SMPTs derived above is applied to the work in references 4, 14, 32, 34 and 35 in Table 2.

Table 2. SMPT scenarios for seeded SMPT experiments which are characterised by a plateau region in solution concentration/supersaturation. The SMPTs are presented in terms of increasing solubility ratio for the transformation.

Compound	SMPT	T (°C)	Solvent[a]	S/S_{eq}[b]	Scenario	Reference
Piracetam	FII → FIII	50	ethanol (s)	1.03	(d)	This work
Tolbutamide	Form I^L →Form II	25	ethanol/water (s)	~1.11	(c)	14
Glycine	α → γ	20	water (ns)	~1.13	(d)	34
Carbamazepine[c]	CBZA → CBZH	16.9	ethanol/ water (s)	~1.21	(d)	35
L-glutamic acid	α → β	45	Water (s)	~1.24	(b)	4
Carbamazepine	FI → FIII	10	methanol (s)	1.39	(b)	This work
Taltireline	α → β	10	water (ns)	~2.00	(d)	33

a - (s): solvent pre-saturated with respect to the solubility of the stable or metastable phase, prior to the addition of the metastable phase, (ns): not pre-saturated. b - estimated from graphical data presented in references. c - phase transformation, anhydrous to dihydrate carbamazepine.

The data set in Table 2 is obviously not intended to be an exhaustive review but some simple observations are worth noting. The data is for a number of different compounds over a range of temperatures and solvents. The specified scenario appears independent of the condition as to whether or not the solvent was saturated prior to addition of the metastable phase. The data shows no trend in

scenario with respect to driving force (approximated using solubility ratio) for the solution mediated transformations.

The thermodynamic driving force for a solution mediated transformation of a metastable polymorph to a stable polymorph is independent of the solvent, and as a first approximation can be described by RTlnS, where S is the solubility ratio of the two forms. For the work reported here, the SMPT of FI to FIII CBZ has a calculated thermodynamic driving force of 0.8 kJ mol^{-1} whereas in the case of PCM the value is 0.05 kJ mol^{-1}, approximately 15 times smaller showing that there is a higher driving force for the SMPT of CBZ. We may note that for the CBZ system, where the driving force is relatively high, there is no appreciable nucleation induction time and the overall rate of transformation is relatively fast. For the PCM system, where the driving force for transformation is relatively low, there is a clear induction time for nucleation and the overall rate of transformation is relatively slow. However, even though the activation energy for a nucleation controlled transformation (i.e. primary nucleation and/or 2-D nucleation growth) decreases with increasing thermodynamic driving force, the comparison of the rate of transformation for different systems cannot only be based on the available driving force. In fact, even for cases in Table 2 belonging to the same transformation scenario, it turns out that a system having a high driving force does not necessarily transform faster than a system having a lower driving force.

The transformation scenarios discussed above may also allude to molecular level mechanistic detail relevant to solution mediated transformations. For example, the solution mediated transformation of α to β L-glutamic acid is known to be facilitated by epitaxial contact between the polymorphic forms during the transformation [36, 37]. Examining the solution concentration in conjunction with the polymorphic composition data for the SMPT of α to β L-glutamic acid shows the immediate transformation from the α to the β form during the plateau region in solution concentration – i.e. there is no detectable induction time for the appearance of the stable β polymorph. Similar solution and solid state behaviour is seen in the case of the SMPT of FI to FIII CBZ presented here. Work is currently being undertaken to investigate if a crystal-crystal epitaxial relationship can be established for the SMPT of FI to FIII CBZ.

CONCLUSION

In situ ATR-FTIR was successfully employed in a calibration free manner to monitor the solution concentration profile during the solution mediated transformations of CBZ and PCM polymorphs. The relative polymorph composition was determined and the solid phase evolution was compared with the solution concentration profile. This experimental approach has allowed the SMPT process to be evaluated in greater detail, generating greater insight into the mechanism controlling these transformations. Both of the SMPTs presented in this work are characterised by a plateau region in solution concentration but when the composition of the solid state is overlaid and compared different behaviours of the solid state exist in this plateau region. In both systems, the overall rate of dissolution of the metastable form is fast compared to the overall rate of growth of the stable form. However, in the SMPT of CBZ, the stable polymorph readily nucleates and grows, but in the case of PCM, there is a considerable induction time prior to nucleation of the stable polymorph.

From a mechanistic point of view four different principal scenarios of polymorphic transformation are defined, based on the nucleation and growth behaviour of the stable phase and the rate of dissolution of the metastable phase. Within this framework on the basis of solution and solid phase information, each specific system can be classified.

ACKNOWLEDGEMENTS

This material is based upon works supported by the Science Foundation Ireland under Grant 07/SRC/B1158.

REFERENCES

(1) Hilfiker, R., Blatter, F., von Raumer, M. in *Polymorphism in the Pharmaceutical Industry*; Hilfiker, R., Ed.;WILEY-VCH: Weinheim, 2006; pp1-3.

(2) Miller, J.; Collman, B. M.; Landon, G. R.; Grant, D. J. W.; Blackburn, A. C., *Pharm. Dev. and Tech.* **2005,** *10*, 291-297.

(3) Gu, C.; Young, J. V.; Grant, D. J. W., *J. Pharm. Sci.* **2001,** *90*, 1878-1890.

(4) Schöll, J.; Bonalumi, D.; Vicum, L.; Mazzotti, M.; Müller, M., *Cryst. Growth Des.* **2006**, *6*, 881-891.

(5) Hao, H.; Su, W.; Barrett, M.; Caron, V.; Healy, A.-M.; Glennon, B., *Org. Process Res. Dev.* **2010,** *14*, 1209-1214.

(6) Doki, N.; Seki, H.; Takano, K.; Asatani, H.; Yokota, M.; Kubota, N., *Cryst. Growth Des.* **2004,** *4*, 949-953.

(7) Wang, F.; Berglund, K. A., *Ind. Eng. Chem. Res.* **2000,** *39* (6), 2101-2104.

(8) Barrett, M.; Hao, H.; Maher, A.; Hodnett, K.; Glennon, B.; Croker, D., *Org. Process Res. Dev.* **2011,** *15*, 681-687.

(9) Cardew, P. T.; Davey, R. J., *Proc. R. Soc. London. Ser. A*, **1985**, *398*, 415-428.

(10) Davey, R. J.; Blagden, N.; Righini, S.; Alison, H.; Ferrari, E. S., *J. Phys. Chem. B* **2002**, *106*, 1954-195.

(11) Rodríguez-Hornedo, N.; Lechuga-Ballesteros, D.; Wu, H.-J., *Int. J. Pharm.* **1992**, *85*, 149-162.

(12) Qu, H.; Kohonen, J.; Louhi-Kultanen, M.; Reinikainen, S.-P.; Kallas, J., *Ind. Eng. Chem. Res.* **2008**, *47*, 6991-6998.

(13) Kelly, R. C.; Rodriguez-Hornedo, N., *Org. Process Res. Dev.* **2009,** *13*, 1291-1300.

(14) Thirunahari, S.; Chow, P. S.; Tan, R. B. H., *Crys Growth Des.* **2011,** *11*, 3027–3038.

(15) Childs, S. L.; Wood, P. A.; Rodriguez-Hornedo, N.; Reddy, L. S.; Hardcastle, K. I., *Crys. Growth Des.* **2009**, *9*, 1869–1888.

(16) Cruz Cabeza, A. J.; Day, G. M.; Motherwell, W. D. S.; Jones, W., *Chem. Comm.* **2007**, *16*, 1600-1602.

(17) Fabbiani, F. P. A.; Byrne, L. T.; McKinnon, J. J.; Spackman, M. A., *CrystEngComm.* **2007**, *9*, 728-731.

(18) Lang, M.; Kampf, J. W.; Matzger, A. J., *J. Pharm. Sci.* **2002**, *91*, 1186-1190.

(19) Arlin, J.-B.; Price, L. S.; Price, S. L.; Florence, A. J., *Chem. Comm.* **2011,** *47*, 7074-7076.

(20) Behme, R. J.; Brooke, D., *J. Pharm. Sci.* **1991**, *80*, 986-990.

(21) Zeitler, J. A.; Taday, P. F.; Gordon, K. C.; Pepper, M.; Rades, T., *ChemPhysChem* **2007**, *8*, 1924-1927.

(22) Fabbiani, F. P. A.; Allan, D. R.; Parsons, S.; Pulham, C. R., *CrystEngComm* **2005**, *7*, 179-186.

(23) Pavlova, A., *Pharmazie* **1979**, *34*, 449-450.

(24) Kuhnert-Brandstatter, M.; Burger, A.; Voellenkelee, R., *Sci. Pharma.* **1994**, *62*, 307-316.

(25) Maher, A.; Croker, D.; Rasmuson, Å. C.; Hodnett, B. K., *J. Chem. Eng. Data* **2010**, *55*, 5314-5318.

(26) Pavlova, A.; Konstantinova, N.; Dashkalov, H.; Georgiev, A., *Pharmazie* **1983**, *38*, 634-637.

(27) Dematos, L. L.; Williams, A. C.; Booth, S. W.; Petts, C. R.; Taylor, D. J.; Blagden, N., *J. Pharm. Sci.* **2007**, *96*, 1069-1078.

(28) McGregor, C.; Saunders, M. H.; Buckton, G.; Saklatvala, R. D., *Thermochimica Acta* **2004**, 417, (2), 231-237.

(29) Barrett, M.; McNamara, M.; Hao, H.; Barrett, P.; Glennon, B., *Chem. Eng. Res. Des.* **2010**, *88*, 1108-1119.

(30) Grzesiak, A. L.; Lang, M.; Kim, K.; Matzger, A. J., *J. Pharm. Sci.* **2003**, *92*, 2260-2271.

(31) Myerson, A. S., *Handbook of Industrial Crystallization*. Butterworth-Heinemann: Woburn, 2002; p 144-146.

(32) Davey, R. J.; Cardew, P. T.; McEwan, D.; Sadler, D. E., *J. Cryst. Growth* **1986**, *79*, 648-653.

(33) Maruyama, S.; Ooshima, H.; Kato, J., *Chem. Eng. J.* **1999,** *75*, 193-200.

(34) Yang, X.; Lu, J.; Wang, X.; Ching, C. B., *J. Raman Spec.* **2008,** *39*, 1433-1439.

(35) Qu, H.; Louhi-Kultanen, M.; Rantanen, J.; Kallas, J., *Cryst. Growth Des.* **2006,** *6*, 2053-2060.

(36) Hammond, R. B.; Pencheva, K.; Roberts, K. J., *Cryst. Growth Des.* **2007**, *7*, 875-884.

(37) Cashell, C.; Corcoran, D.; Hodnett, B. K., *Chem. Comm.* **2003**, 374-375.

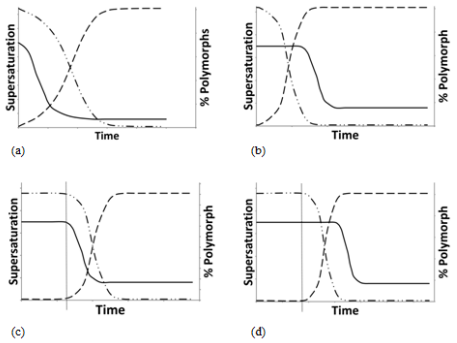

Solution and solid state composition were examined for the solution mediated polymorphic transformation of carbamazepine, piracetam and other compounds in the literature. Comparison of solution and solid state information for a solution mediated transformation enables the transformation to be classified as behaving in accordance with one of four principal scenarios.